TWO-PHOTON ABSORPTION MEASURED IN THE PRESENCE OF STRONG ONE-PHOTON SATURATION IN CUMULENE-CONTAINING POLYMER

R. K. Meyer*, M. Shkunov, R.E. Benner†, W. Gellermann, and Z. V. Vardeny,
Departments of Electrical Engineering† and Physics
University of Utah, Salt Lake City, Utah 84112,

J. Lin, and T. J. Barton,
Department of Chemistry
Iowa State University, Ames, Iowa 50011

Abstract

The Z-scan technique is used to extract the real and imaginary third order nonlinear susceptibilities, $Re\chi^{(3)}$ and $Im\chi^{(3)}$, respectively. A series of Z scans were conducted at 590 nm (near one-photon resonance) on a cumulene-containing polymer, poly(p-phenylene-1,4-diphenyl-1,2,3-butatriene) or PPC3, prepared in solution. At very high peak focal point intensities two-photon absorption is seen superimposed on a one-photon saturation signature in open aperture Z scans. A negative real third-order nonlinear susceptibility is also observed in closed aperture Z scans. We describe a procedure to extract the desired third-order nonlinear susceptibilities by conducting Z scans at various peak focal point intensities and then fitting the results by adjusting $Re\chi^{(3)}$ and saturation intensity. Molecular second hyperpolarizability, is calculated to be $(-1.4+2.2i)\times10^{-29}$ esu which is almost 40 times larger than that measured in a monomer equivalent, and scaling nonlinearly with chain length. Z scans were also conducted at 780 nm (below one-photon resonance) on PPC3 and also gives a molecular second hyperpolarizability that is greater than that seen in the monomer. The higher value of molecular second hyperpolarizability measured near one-photon resonance is attributed to the existence of a real state at the first transition in a two-photon process. The extent of the exciton wave function obtained from the saturation intensity, is 60 Å, larger than a single repeat unit.

Keywords: molecular second hyperpolarizability, one-photon saturation, polymer solution, cumulenes, chain length.

1. Introduction

Comparatively assessing the size of third order nonlinear optical susceptibilities, $\chi^{(3)}$, in π-conjugated polymers is important for the identification of materials that have potential engineering device application and in determining the physical attributes that enhance the nonlinear index of refraction, n_2. It has been predicted and theorized that the number of monomer repeat units has a strong effect in this regard.[1] This trend has, in fact, been verified in the case of thiophene oligomers.[2] The obvious approach is to perform a systematic study of polymer nonlinearities as a function of the number of repeat units. Zhao et al., using this approach, found a drastic increase in real $\chi^{(3)}$ with repeat unit in thiophene oligomers.[2] However, for the case of highly conjugated cumulene structures, the results were inconclusive.[3] The π-conjugated backbone of the cumulene polymers is formed by a series of carbon double bonds (see Fig. 2, inset) as opposed to the alternating single and multiple bonds found in other π-conjugated polymers such as polydiacetylene. Conjugation in cumulene arises from the π orbitals being arranged, in an alternating fashion, parallel and perpendicular to the molecular plane. When the number of carbon double bonds is odd, the two end π orbitals are oriented in the plane of the cumulene molecular frame which effectively extends the conjugation through the attached groups.[4] The resulting π electron delocalization, in turn, increases $\chi^{(3)}$ or, equivalently, the orientationally averaged molecular second hyperpolarizability, γ.

To further investigate these theoretical predictions, nonlinear optical measurements on a cumulene-containing polymer were conducted and compared to values obtained for the monomer species. Breakthroughs in synthesis,[5, 6] enabled the acquisition of multiple repeat-unit, cumulene-containing polymers with various numbers of carbon-carbon double bonds. Measurements were conducted on poly(p-phenylene-1,4-diphenyl-1,2,3-butatriene), or PPC3. This polymer has three carbon double bonds, with an average of five monomer repeat units.[5]

There are several valid techniques for measuring $\chi^{(3)}$ of polymers. Although the degenerate four-wave mixing (DFWM) technique was used previously in the monomer investigations[3], we chose to use the Z-scan technique[7], which enables determination of both the real (Re) and imaginary (Im) $\chi^{(3)}$ values and their respective signs. Furthermore, Z scan allows separation of effective nonlinear susceptibilities caused by one-photon saturation from actual two-photon processes. This capability is especially important when investigating a material near one-photon resonance where large saturation effects are expected.[8]

2. Z-Scan Technique for Solutions

The Z-scan technique is based on the self-focusing/defocusing effects in a nonlinear material. A laser beam is focused by a lens onto a nonlinear material of interest. The divergent beam after the sample is observed by a photodetector. By moving the sample back and forth through the focal point of the lens, the impinging intensity is effectively varied, resulting in intensity-dependent changes in transmission and spot size at the photodetector. Changes in the real index of refraction, n_2 proportional to $\mathrm{Re}\chi^{(3)}$ result in focusing (positive) or defocusing (negative). Focusing effects are measured by placing an aperture in front of the detector and observing the transmission through the aperture as a function sample position. Nonlinear absorption ($\mathrm{Im}\chi^{(3)}$), on the other hand, is obtained by allowing the entire beam to irradiate a near-field detector, thereby detecting the changes in absorption. The two effects are measured simultaneously by placing a beam splitter immediately behind the sample. Using the approximation described by Sheik-bahae, et al.,[7] the value of n_2 can be extracted directly by measuring the change in transmission between the peak and the valley signature of the typical closed aperture Z scan. Using the change in transmission ΔT, n_2 and $\mathrm{Re}\chi^{(3)}$ can be calculated using

$$n_2(\mathrm{cm}^2/\mathrm{W}) \cong \frac{\Delta T \lambda}{(.406)(2\pi)(I_o)L_{\mathrm{eff}}}, \tag{1a}$$

and

$$\mathrm{Re}\,\chi^{(3)}(\mathrm{esu}) = \frac{n_o c}{12\pi^2} n_2(\mathrm{cm}^2/\mathrm{W})(10^{-7}), \tag{1b}$$

where, I_o is the peak on-axis intensity of the excitation laser, λ is the free-space wavelength of the excitation laser, c is the speed of light, n_o is the real linear index of refraction, and L_{eff}, the effective length is given by $L_{\mathrm{eff}} = (1 - e^{-\alpha_o L})/\alpha_o$, with L being the actual length and α_o the linear absorption (cm^{-1}). The nonlinear absorption α_2 is obtained by fitting the open aperture scan using the equation,

$$T(z) = \sum_{m=0}^{\infty} \left\{ \left[\frac{-\alpha_2 I_o L_{\mathrm{eff}}}{1 + z^2/z_o^2} \right]^m \Big/ (m+1)^{3/2} \right\}, \tag{2a}$$

and

$$\mathrm{Im}\,\chi^{(3)}(\mathrm{esu}) = \frac{n_o c \lambda}{48\pi^2} \alpha_2(\mathrm{cm}/\mathrm{W})(10^{-7}) \tag{2b}$$

as described in Reference 7. The complex $\chi^{(3)}$ of a material is completely specified in this manner. The high peak powers (typically around 20 GW/cm^2) required for Z scan often leads to permanent material damage as a result of heating. A dilute solution with the desired material as the solute, enables us to avoid this thermal damage. The complex $\chi^{(3)}$ measured for a solution then becomes, assuming noninteracting particles, an effective $\chi^{(3)}$ given by

$$\chi^{(3)}_{\mathrm{eff}} = L^4(N_{\mathrm{solute}}\gamma_{\mathrm{solute}} + N_{\mathrm{solvent}}\gamma_{\mathrm{solvent}}) \tag{3}$$

where N_{solute} and $N_{solvent}$ are the number densities (cm^{-3}) of the solute and solvent, respectively, and γ_{solute}, and $\gamma_{solvent}$ are the molecular second hyperpolarizabilites ($\chi^{(3)}$ per molecule) of the solute and solvent, respectively. The local field factor, L, is given by

$$L = \left(\frac{\left(n^2 + 2\right)}{3} \right). \tag{4}$$

By analogy the effective linear susceptibility, $\chi^{(1)}$ can be written as

$$\chi_{eff}^{(1)} = L(N_{solute}\alpha_{solute} + N_{solvent}\alpha_{solvent}) \tag{5}$$

where, α_{solute} and $\alpha_{solvent}$ are the molecular polarizabilities of the solute and solvent, respectively. The linear susceptibility will be important when strong one-photon saturation effects are present.

When a material exhibits both strong nonlinear absorption and nonlinear refraction, the reduced-aperture Z scan measures the combined effect. However, the open-aperture Z scan, since it is insensitive to phase changes, measures only the nonlinear absorption. The observed effect on the reduced-aperture Z scan is to make it no longer antisymmetric (see Fig.3b). The symmetric nonlinear absorption transmission changes and the antisymmetric nonlinear refraction transmission changes are effectively mixed in a multiplicative manner. Under these circumstances, the reduced-aperture and open-aperture approximation techniques can still be employed. It was found[7] that, by dividing the reduced-aperture data by the open-aperture data, the nonlinear absorption effects could be removed to within ± 10% accuracy.

3. Resonant Enhancement

The two-photon absorption (TPA) process and the related nonlinear index of refraction are enhanced by the existence of real states with strong dipole coupling at energies near that of the excitation wavelength. Since Z scan is an intensity-dependent effect there are two possible processes involving four photons at the same wavelength; TPA and one-photon saturation (see Fig. 1).

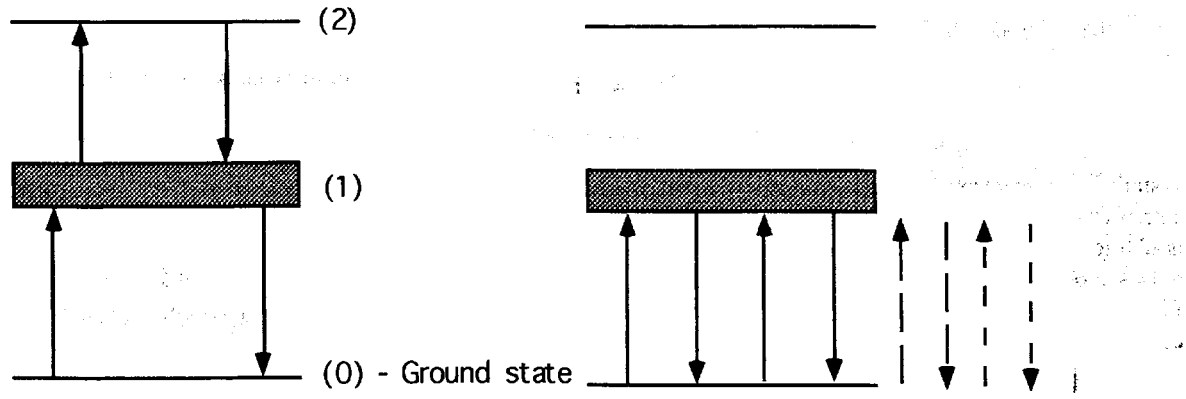

Figure 1. Two-step absorption process mediated by long-lived triplet state at level one. Heavy shading of level one indicates population accumulation. Dashed and short dashed lines indicate fifth and seventh order terms involving six and eight photons, respectively.

The measured $\chi^{(3)}$ is a combination of the two effects with TPA contributing a positive $\chi^{(3)}$ term and saturation contributing a negative $\chi^{(3)}$. The negative $\chi^{(3)}$ contribution, arising from saturation, can be understood by considering a Taylor series expansion of the saturation equation for a two level system.

$$\chi^{(1)}(I) = \chi^{(1)}\left[1+\frac{I}{I_s}\right]^{-1/2} \approx \chi^{(1)}\left[1-\frac{1}{2}\frac{I}{I_s}+\frac{3}{4}\frac{I^2}{I_s^2}-\ldots\right] \qquad (6)$$

where, $\chi^{(1)}(I)$ is the complex intensity-dependent linear susceptibility, $\chi^{(1)}$ is the complex low-intensity linear susceptibility, and I_s is the saturation intensity. The second term, $\frac{\chi^{(1)}}{2I_s}$, is an effective negative $\chi^{(3)}$ term. As intensity increases the higher order terms become important leading to alternating sign fifth and seventh order nonlinear susceptibilities.

It is evident that a real state such as $1B_u$ at level one will exhibit both a large TPA $\chi^{(3)}$ ($\chi^{(3)}_{TPA}$) and a large effective negative $\chi^{(3)}$ from the process in Fig. 1b. Nonlinear processes enhanced by resonances, while large, are not useful for many engineering applications because of the attendant linear or nonlinear absorption which results in heating and reduces the interaction length. Moreover, the effect of resonances complicates the measurement and comparison of $\chi^{(3)}$ in π-conjugated polymers since the resonances vary depending on factors such as chain length, bond length alternation, overlap/geometry of the π-orbitals, etc. Unfortunately, it is not feasible in advance to determine all possible resonances since this would require the painstaking process of obtaining the two-photon absorption spectrum. However, by conducting Z scan at excitation energies near the easily obtained one-photon resonance of each polymer and can thereby compare $\chi^{(3)}$s under equivalent resonant conditions. There are two important advantages in using this method with regards to resonances in π-conjugated polymers: 1) We know in advance where the one-photon resonances are from simple linear absorption measurements, and 2) considerable theoretical[9-11] and experimental[12-14] evidence suggests that strong two-photon resonances (i.e. mA_g) exist around $1.2E_{gap}$ ensuring that we do not have an additional two-photon resonance at twice the excitation energy. The enhancement of the TPA process as a result of the strong one-photon absorption is accounted for by comparing the figure of merit,

$$\kappa = \mathrm{Re}\gamma / \mathrm{Im}\alpha, \qquad (7)$$

rather than γ alone. In Eq. (7) α is the molecular polarizability rather than the linear absorption.

4. Experiment

To obtain the high peak powers required for Z-scan experiments, we employed a regeneratively pumped dye amplifier system.[15] A Quantronix frequency-doubled Nd:YAG laser provided excitation for a synchronously pumped dye laser. The dye amplifier system was pumped through regenerative amplification of the Nd:YAG master oscillator and subsequent frequency doubling. The high repetition rate dye laser pulses were amplified approximately 50,000 times, resulting in 10 psec, 250 Hz pulses at 60 GW/cm^2 peak intensity. To verify the nonresonant γ measured at 590 nm, additional Z scans were performed on PPC3 at 780 nm, using an amplified Ti:sapphire system. The laser beam was focused by a 10 cm focal length lens into the cuvette. The diverging beam after the sample was observed by a large area silicon detector (Si:PIN 10 DP, UDT).

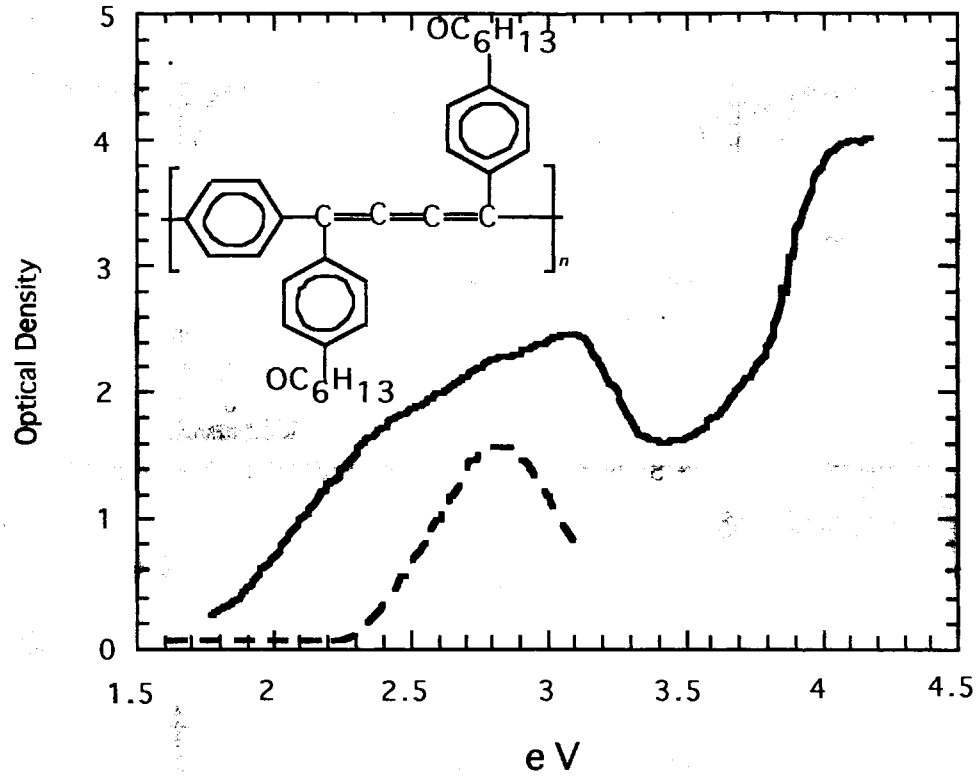

Figure 2. Linear absorption spectrum of the cumulene polymer PPC3 (solid line) and its monomer equivalent (dashedline) in chloroform solution.

Reduced aperture Z scans on CS_2 were conducted in order to calibrate and validate the system leading to a $Re\chi^{(3)} \cong 2.0 \times 10^{-12}$ esu, within 10% of published values.[16-18] The linear absorption spectrum of PPC3 and its monomer equivalent have absorption edges beginning near 1.5 eV (820 nm) and 2.14 eV (580 nm), respectively, as illustrated in Fig 2. Open and reducedaperture scans were then conductedon a 9.4×10^{-4} g/cm^3 and 3.1×10^{-3} g/cm^3 chloroform solution of PPC3 in a 1 mm thick glass cuvette at wavelengths of 590 nm (2.1 eV) and 780 nm (1.58 eV), respectively. Z scans were also conductedon a 4.8×10^{-3} g/cm^3 solution of the monomer equivalent at 590 nm.

The Z-scan open and reducedaperture results for PPC3 at 590 nm and at 780 nm are depictedby open circles in Figs. 3 and 4 respectively. Z scans for the monomer equivalent at 590 nm are illustrated in Figure 5. The open aperture scan for PPC3 (Fig. 3(a)) clearly indicates the presence of one-photon saturation, as exhibited by an increase in transmission as z approaches zero from the left or right. The reducedaperture scan in PPC3 (Fig. 3(b)) is dominated by the change in absorption, but also exhibits, because of its apparent asymmetry, a change in index of refraction. The open aperture scan for the monomer at 590 nm and PPC3 at 780 nm, in contrast, are devoid of this saturation effect, as would be expected from the weak linear absorption at 590 nm for the monomer and at 780 nm for PPC3 (Fig. 2). We, therefore, obtain $Re\chi^{(3)}$ and $Im\chi^{(3)}$ by equations (1) and (2), respectively; $\chi^{(3)}_{mono}(590\,nm) = (-7.5 + 1.1i) \times 10^{-13}$ esu and $\chi^{(3)}_{PPC3}(780\,nm) = (-4.2 + .52i) \times 10^{-12}$ esu.

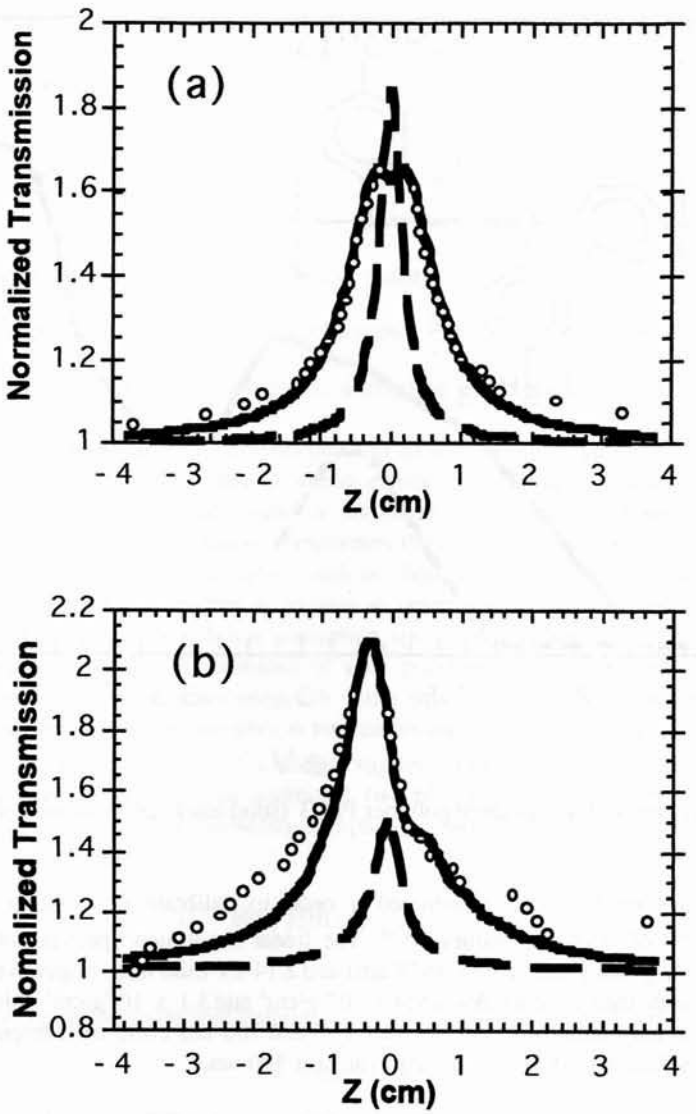

Figure 3. Open circles are Z scans conducted at I=0.57 GW/cm^2 on a 9.4 x10^{-4} g/cc PPC3 solution. Dashed lines are fits using a model which includes $\chi^{(3)}$ only. Solid lines show a fit with a more complete model Eqs. (9a) and (9b). (a) Open-aperture Z scan. (b) Reduced-aperture Z scan

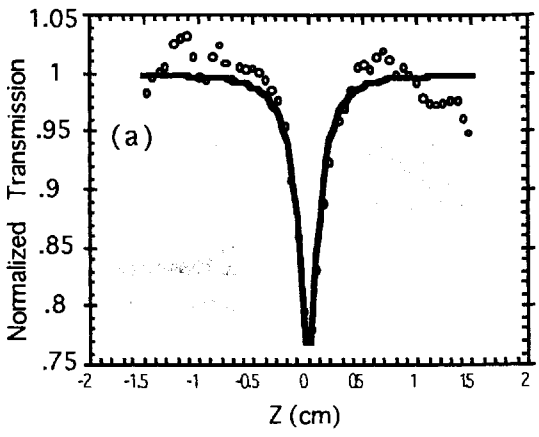

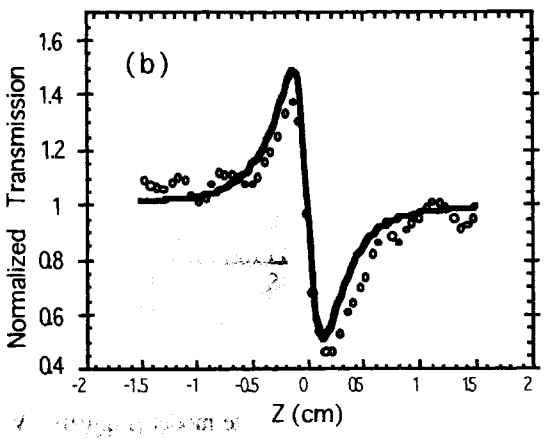

Figure 4. Open and reduced-aperture Z scans on PPC3 at 780 nm. Solid line indicates best fit based on calculated values for n_2 and α_2.
(a) Reduced-aperture Z scan. (b) Open-aperture Z scan.

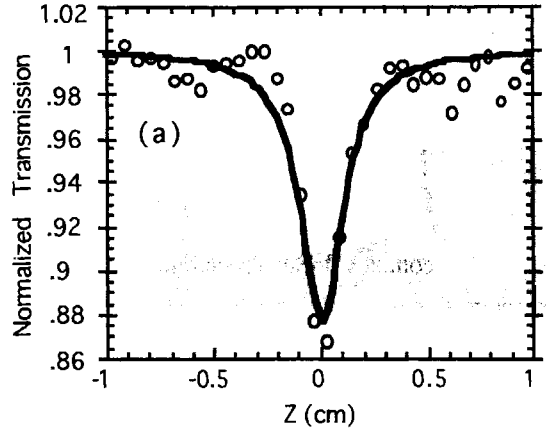

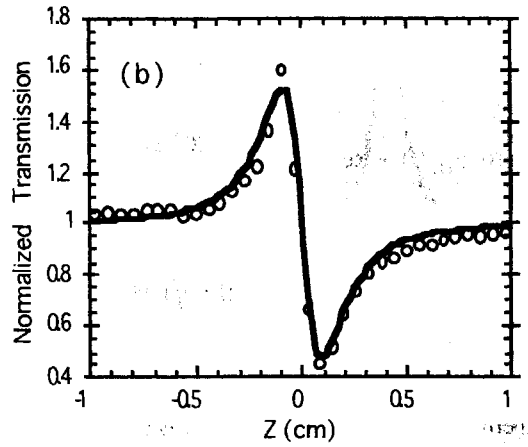

Figure 5. Open and reduced-aperture Z scans on PPC3 monomer equivalent. Solid line indicates best fit based on calculated values for n_2 and α_2.
(a) Reduced-aperture Z scan. (b) Open-aperture Z scan.

5. Analysis and Discussion

5.1 Saturation

Using the simple first-order approximation technique outlined in Ref. ([7]) to calculate real $\mathrm{Re}\chi^{(3)}$ and $\mathrm{Im}\chi^{(3)}$ for PPC3, resulted in the fits illustrated by the dashed lines in Fig. 3, which are clearly unsatisfactory. The fits improve by assuming a larger beam waist or by including alternating-sign, higher-order nonlinearities, $+\mathrm{Re}\chi^{(3)}$, $-\mathrm{Re}\chi^{(5)}$, $+\mathrm{Re}\chi^{(7)}$, etc.[12] The higher order χs arise from the saturation effect, which is so large as to invalidate truncation of the Taylor series expansion in Equation (6). [8]

We tested the validity of the saturation equation by conducting open aperture Z Scans at various laser intensities (Fig. 6). If saturation effects dominate, we would expect to see a nonlinear increase in maximum transmission at z=0 as I increases. However, as clearly seen in Fig. 6c, a dip appears at the highest intensities, indicating the presence of a nonlinear absorption process.

To account for this nonlinear process, we must include a positive two-photon absorption, $\chi^{(3)}_{TPA}$, term. The adjusted model, comprised of saturation effects and TPA $\chi^{(3)}$ gives an intensity-dependent susceptibility, $\chi_{eff}(I)$,

$$\chi_{eff}(I) = \chi^{(3)}_{TPA} I + \frac{\chi^{(1)}_{eff}}{(1 + I/I_s)^{1/2}} \qquad (8)$$

where $\chi^{(1)}_{eff}$ is the effective complex linear susceptibility of the solute-solvent combination. For the case where the solvent and solute are non-interacting molecules and the excitation wavelength is far from resonances of the solvent, $\chi^{(1)}_{eff}$ is the sum of the solvent and solute complex linear susceptibilities as in Equation (5). From the refractive index of chloroform (n=1.444), we calculate $\mathrm{Re}\,\chi^{(1)}_{solvent} = 8.6 \times 10^{-2}$ esu, and, since the chloroform solvent is transparent at 590 nm, $\mathrm{Im}\,\chi^{(1)}_{solvent} = 0$. Also, from the PPC3 linear absorption at 590 nm and 780 nm, we calculate $\mathrm{Im}\,\chi^{(1)}_{solute} = 2.9 \times 10^{-5}$ esu, and $\mathrm{Im}\,\chi^{(1)}_{solute} = 1.9 \times 10^{-5}$ esu, respectively. Thus, we arrive at two equations that describe the reduced-aperture ($T(z) \propto \mathrm{Re}\,\chi^{(3)}_{eff} + \mathrm{Im}\,\chi^{(3)}_{eff}$) and open-aperture ($T(z) \propto \mathrm{Im}\,\chi^{(3)}_{eff}$) Z scans.

$$\mathrm{Re}\,\chi_{eff}(I) = \mathrm{Re}\,\chi^{(3)}_{solute} I + \frac{\mathrm{Re}\,\chi^{(1)}_{solute} + \mathrm{Re}\,\chi^{(1)}_{solvent}}{(1 + I/I_s)^{1/2}}, \qquad (9a)$$

and

$$\mathrm{Im}\,\chi_{eff}(1) = \mathrm{Im}\,\chi^{(3)}_{solute} I + \frac{\mathrm{Im}\,\chi^{(1)}_{solute}}{(1 + I/I_s)^{1/2}}. \qquad (9b)$$

In equations (8a) and (8b) we neglect the contributions to $\chi^{(3)}$ from the chloroform solvent since it is less than 10% ($\approx 10^{-14}$ esu) the value of the overall effective $\chi^{(3)}$ according to our Z-scan measurements.

Open-aperture Z-scan simulations were calculated to test the validity of this more complete model [Eq. (9)]. With parameters (peak power and beam waist at focal point) identical to the actual Z scans, we obtained the simulations depicted in Figure 7. The overall similarity between Figs. 6 and 7 validates our model.

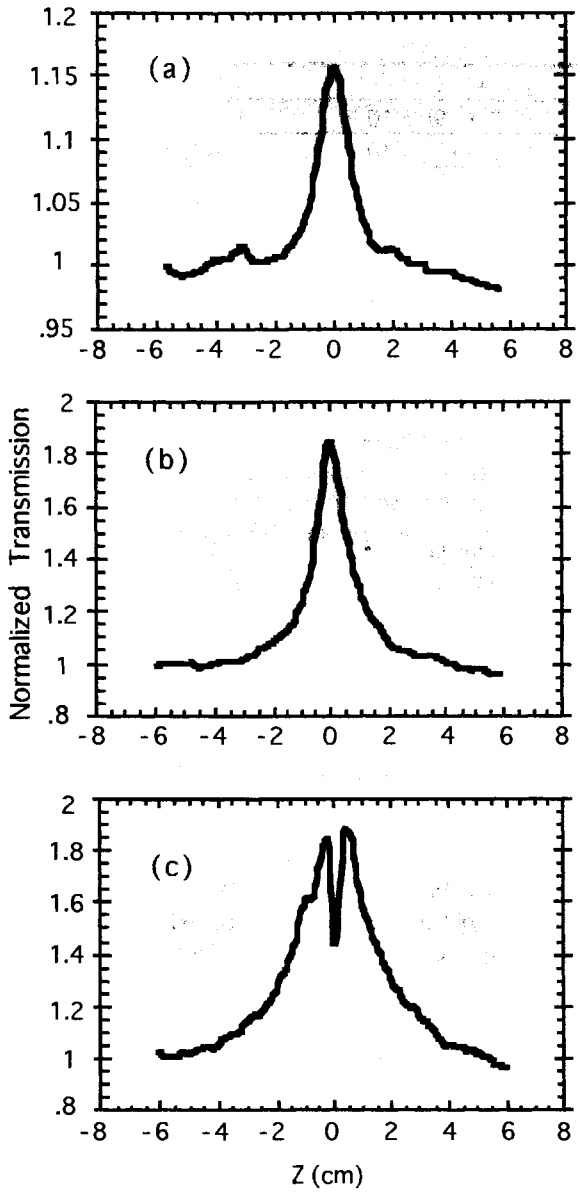

Figure 6. Open-aperture Z scans of PPC3 solution with varying I_o: (a) I =0.67 GW/cm^2, (b) I = 8.9 GW/cm^2, and (c) I = 64 GW/cm^2.

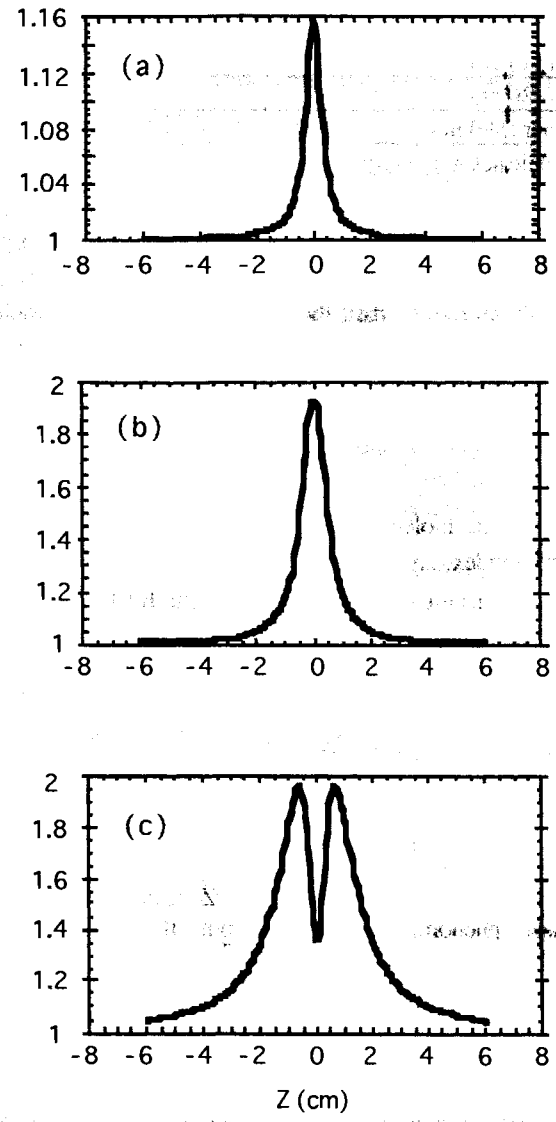

Figure 7. Simulations of open-aperture Z scans shown in Fig. 6 using the more complete model Eqs. (9a) and (9b). The values of I_o in (a) to (c) are the same as in Fig. 6.

Applying this model, we obtained the curve fits indicated by the solid lines in Fig. 3. The basic procedure employed a simplex least squares method to fit the open aperture scan first by adjusting the saturation intensity, I_s, and $\mathrm{Im}\chi^{(3)}_{TPA}$. In this manner we obtained $I_s = 9 \times 10^7$ W / cm^2 and $\mathrm{Im}\chi^{(3)}_{NR} = 9.6 \times 10^{-12}$ esu. We then fit the closed aperture scans using these values and adjusting $\mathrm{Re}\chi^{(3)}_{TPA}$ and $\mathrm{Re}\chi^{(1)}_{solute}$, respectively. We found $\mathrm{Re}\chi^{(3)}_{NR} = -6.2 \times 10^{-12}$ esu and $\mathrm{Re}\chi^{(1)}_{solute} = 1.2 \times 10^{-6}$ esu. Table I summarizes the experimentally determined linear and nonlinear susceptibilities.

Table 1. Summary table of measured linear and third order optical susceptibilities of polymer and monomer solutions.

	Concentration (g/cm^3)	$\chi^{(1)}$ (esu)	$\chi^{(3)}$ (esu)
PPC3 (590 nm)	9.4×10^{-4}	$(.12+2.9i) \times 10^{-5}$	$(-6.2+9.6i) \times 10^{-12}$
PPC3 (780 nm)	3.1×10^{-3}	$(????+1.9i) \times 10^{-5}$	$(-4.2+.52i) \times 10^{-12}$
Monomer (590 nm)	4.8×10^{-3}	$(????+6.7i) \times 10^{-6}$	$(-7.5+1.1i) \times 10^{-12}$

???? - indicates a quantity that was not measured.

5.2 Molecular Second Hyperpolarizabilities and Polarizabilities

From the $\chi^{(3)}$ data, the orientationally-averaged molecular hyperpolarizability, γ, is also calculated for the monomer and polymer, respectively, using the equation,[4]

$$\gamma = \frac{\chi^{(3)}}{N_0 L^4}, \tag{11}$$

where N_0 is the molecular concentration and L is the Lorentz local field factor given by $L = (n^2 + 2)/3$. Substituting the refractive index, n, for chloroform, yields, $\gamma_{TPA}(590nm) = (-1.4 + 2.2i) \times 10^{-29}$esu for the PPC3 polymer and $\gamma_{mono}(590nm) = (-5.4 + 0.39i) \times 10^{-32}$esu for the monomer. Furthermore, it is possible to calculate the orientationally-averaged molecular polarizability, α, from $\chi^{(1)}$ using the relationship

$$\alpha = \frac{\chi^{(1)}}{N_0 L}, \tag{12}$$

which gives $Re(\alpha)=1.7 \times 10^{-22}$ esu.

For comparative purposes, additional Z scans were conducted on a PPC3 solution at 780 nm employing the amplified Ti:sapphire laser system. Z scans at this wavelength were devoid of saturation effects, exhibiting third-order nonlinear phenomena only in both the open and reduced aperture scans. Based on this Z-scan data, a $\gamma_{TPA}(780nm) = (-2.4 + 0.22i) \times 10^{-30}$esu was calculated. Thus, the value of the real part of γ_{TPA} measured at 780 nm is about 1/6 the value deduced from the γ_{TPA} previously calculated at 590 nm. The calculated hyperpolarizabilities and polarizabilities are summarized in Table 2.

Table 2. Hyperpolarizabilities and polarizabilites calculated from Z-scan data.

Quantity* measured (wavelength of measurement)	Complex value of quantity (esu)	κ Figure of Merit
$\gamma_{monomer}$(590 nm)	$(-5.4+0.39i) \times 10^{-32}$	6.7×10^{-9}
γ^{TPA}_{PPC3}(590 nm)	$(-1.4+2.2i) \times 10^{-29}$	8.2×10^{-8}
γ_{PPC3}(780 nm)	$(-2.4+0.22i) \times 10^{-30}$	7.1×10^{-8}
$\alpha_{monomer}$(590 nm)	$(????+5.8i) \times 10^{-25}$	
α_{PPC3}(590 nm)	$(0.68+1.7i) \times 10^{-22}$	
α_{PPC3}(780 nm)	$(????+.34i) \times 10^{-22}$	

*TPA indicates a nonresonant γ with saturation effects mathematically excluded.

???? - indicates a quantity that was not measured.

5.3 Exciton Size

Based on the phenomenological argument of Green et al., the excitonic wave function extent, ε, can be estimated as[19]

$$\varepsilon = \frac{1}{\mathcal{N}_s}, \tag{13}$$

where $\mathcal{N}_s$ is the linear saturation density. The thrust of the argument is that for an exciton size of ε and molecular chain length L, there can only be L/ε excitons. This is the one-dimensional analog to the phase-space filling model in multiple quantum well (MQW) semiconductors presented by Schmitt et al..[20] In the case of polymers, however, the phase space is one-dimensional, and the optically active exciton will be formed by band states with $k<2\pi/\varepsilon$ (where k is the wave propagation constant).[21] If the exciton is large enough, only one will be required to fill the phase space. The wave functions begin to overlap when the phase space becomes filled and further excitonic formation will be prevented unless accompanied by downward transitions. This can also be understood in terms of the fermion characteristics of the excitons' constituents (electrons and holes) where, by the exclusion principle, the exciton transitions will begin to saturate when overlap occurs. The linear number density for saturation is then given by the reciprocal of Eq. (13).

Now using I_s previously calculated from the Z-scan data, an expression is obtained for the volumetric saturation density, N_s,

$$N_s = \frac{I_s \tau_p \alpha_0}{\hbar\omega}, \tag{14}$$

where τ_p is the laser pulse width, α_0 is the zero intensity linear absorption, and ω is the frequency of the excitation beam. Taking into account the solution density and the percentage of that solution occupied by a single chain length gives, for the linear exciton saturation density on a chain,

$$\mathcal{N}_s = \frac{N_s}{N_0 L}, \tag{15}$$

where L refers to the average molecular chain length and N_0 is the number density of the solute (cm^{-3}), PPC3. Therefore, from Eq. (13) the exciton wave-function extent is given by

$$\varepsilon = \frac{1}{\mathcal{N}_s} = \frac{N_0 L}{N_s} \tag{16}$$

From the value of I_s previously determined, the exciton wave function extent is calculated as 60 Å for the $1B_u$ exciton in PPC3. This is much larger than the PPC3 monomer unit length of about 10 Å, and indicates exciton delocalization over several monomers.

6. Conclusion

Using the Z-scan technique near one-photon resonance on polymers in solution gives good comparative values for γ and $\chi^{(3)}$, determines the extent of π-conjugation, and enables calculation of the real molecular polarizability, α. At 590 nm, the measured $\mathrm{Re}\gamma_{TPA}$(590 nm) of -1.4 x 10^{-29} esu for PPC3 is 260 times larger than the value we measured for its monomer equivalent, $\mathrm{Re}\gamma_{mono}$(590 nm)= -5.4 x 10^{-32} esu. According to the theoretical calculations of Ref. ([22]), γ should increase rapidly with chain length. Optical nonlinear results for oligothiophenes indicate a power law dependence for γ , $\gamma \propto N_0^p$, where N_0 is the number of repeat units and $p \approx 4.6$.[23] Based on the measured enhancement factor of 260 for PPC3 (N_0=5),

we calculate, for cumulenes, p = 3.5. The calculated value for p is in agreement with p values for other conjugated polymers.[16] More importantly, however, the κ [Eq. (7)] figure of merit for measurements on PPC3 at 590 nm and 780 nm are approximately the same, and together, more that 12 times larger than κ for the monomer. Our experimental results thus indicate that the excited state wavefunction in cumulenes becomes more delocalized with longer chain lengths, which is also in agreement with other π-conjugated polymers. Moreover, the calculated exciton size D = 60 Å, which is much larger than the size of the PPC3 monomer, indicates that the π electrons are, indeed, delocalized beyond a single monomer repeat unit.

The work at the University of Utah was supported in part by ONR Grant No. N00014-94-1-0853, DOE grant FG-03-96ER45490, and from the University of Utah Research Committee. Ames Laboratory is operated by Iowa State University for the U.S. Department of Energy under contract W-7405-Eng-82. The work at Iowa State University was supported by NSF (DMR A2-22947).

7. References

1. R. F. Shi, Q. L. Zhou, J. R. Heflin, *et al.*, Noninear Optics **6**, 305-316 (1994).
2. M. Zhao, B. P. Singh, and P. N. Prasad, J. Chem. Phys. **89**, 5535-5541 (1988).
3. I. Kminek, J. Klimovic, and P. N. Prasad, Chem. Mater. **5** (1993).
4. P. N. Prasad and D. J. Williams, *Introduction to Nonlinear Optical Effects in Molecules and Polymers* (Wiley, New York, 1991).
5. J. Lin, in *Chemistry* (Iowa State University, Ames, 1995), p. 224.
6. J. Lin, S. Ijadi-Maghsoodi, T. J. Barton, *et al.*, Polymer Preprint **35**, 832-833 (1994).
7. M. Sheik-Bahae, A. A. Said, T. Wei, *et al.*, IEEE J. of Quant. Electronics **26**, 760-769 (1990).
8. L. Yang, R. Dorsinville, Q. Z. Wang, *et al.*, Optics Letters **17**, 323-325 (1992).
9. D. Guo, S. Mazumdar, and S. N. Dixit, Synthetic Metals **49**, 1-11 (1992).
10. D. Guo, in *Physics* (Univ. of Arizona, Tucson, 1993), p. 107.
11. P. C. M. McWilliams, G. W. Hayden, and Z. G. Soos, Phys. Rev. B **43**, 9777-9791 (1991).
12. U. Lemmer, R. Fischer, J. Feldmann, *et al.*, Chemical Physics Letters **203**, 28-32 (1993).
13. S. A. Jeglinski, Z. V. Vardeny, Y. Ding, *et al.*, Mol. Cryst. Liq. Cryst. **256**, 87-96 (1994).
14. C. J. Baker, O. M. Gelsen, and D. D. C. Bradley, Chemical Physics Letters **201**, 127-131 (1993).
15. I. N. Duling, T. Norris, T. Sizer, *et al.*, J. Opt. Soc. Am. **2**, 616 (1985).
16. P. Thomas, A. Jares, and B. P. Stoicheff, IEEE J. of Quantum Electronics , 493-494 (1974).
17. M. J. Soileau, W. E. Williams, and E. W. V. Stryland, IEEE J. of Quant. Electr. **19**, 731-735 (1983).
18. K. Sala and M. C. Richardson, Phys. Rev. A. **12**, 1036-1047 (1975).
19. B. I. Greene, J. Orenstein, R. R. Millard, *et al.*, Phys. Rev. Lett. **58**, 2750-2753 (1987).
20. S. Schmitt-Rink, D. S. Chemla, and D. A. B. Miller, Phys. Rev. B **32**, 6601-6609 (1985).
21. C. Kittel, *Introduction to Solid State Physics* (Wiley and Sons, Inc., New York, 1986).
22. P. Chopra, L. Carlacci, H. F. King, *et al.*, J. Phys. Chem. **93**, 7120-7130 (1989).
23. H. Thienpont, G. L. J. A. Rikken, E. W. Meijer, *et al.*, Phys. Rev. Lett. **65**, 2141-2144 (1990).